X-RAY COMPUTED TOMOGRAPHY-BASED FE-HOMOGENIZATION OF SHEARED ORGANO SHEETS

O. Shishkina[1*], A. Matveeva[1*], S. Wiedemann[2], K. Hoehne[2] , M. Wevers[3], S. V. Lomov[3] , L. Farkas[1]

[1]Siemens Industry Software NV, Leuven, Belgium
[2]INPRO Innovationsgesellschaft für fortgeschrittene Produktionssysteme in der Fahrzeugindustrie mbH, Berlin, Germany
[3]KU Leuven, Department of Materials Engineering (MTM), Leuven, Belgium
*Joined first co-authors: oxana.shishkina@siemens.com; anna.matveeva@siemens.com

Keywords: micro-CT, sheared fabric, voxel models, FE homogenization

Abstract
In this work, finite element models of thermoplastic woven organo sheets sheared to various angles were created from X-Ray computed tomography images using voxel-based approach. Virtual assessment of the effect of shear on the homogenized composite elastic properties shows a good agreement with the experimental results.

1. Introduction and motivation

Manufacturing of complex shape thermoplastic composite parts can be achieved through thermoforming the composite into the desired shape. The drawback of such a processing technology lies in local changes of the internal structure of the composite, e.g. thickness variation and reinforcement misorientation mainly due to the shear, a deformation mechanism typical for a thermoplastic woven composite during thermoforming [1-2]. Thus, accurate simulations of the composite parts should take into account the manufacturing-induced local variabilities in the composite geometry, which affect the stiffness values locally and, consequently, the mechanical properties of the composite part itself.

The effect of shear on the composites stiffness properties was previously assessed using both analytical formulations and finite element (FE) analysis [3]. The results showed that the analytical shearing did not capture the changes in the fabric geometry accurately. Consequently, a FE model of the sheared organo sheet was also built based on idealized geometry. In the referenced paper [3], it was concluded that for largely sheared configurations severe interpenetrations blocked the generation and computation of FE models.

As an alternative to "idealized models", a voxel-based approach has been developed in [4-5] for a direct conversion of three-dimensional (3D) images of real composites microstructure into finite element models, which are acquired using X-ray micro-computed tomography (micro-CT). Micro-CT technique shows great potential for improving the understanding of the structural features of composite materials, their influence on materials performance and changes in those features during composites' manufacturing, exploitation and failure [6-10].

In this work, the micro-CT-based modeling approach was used to estimate the effect of shear on the mechanical performance of the sheared organo sheets. On one hand, unit cell mesostructure of the sheared composites was characterized using micro-CT and, further, converted into the representative FE

voxel model. On the other hand, a series of tensile tests were performed to determine the elastic modulus of the sheared organo sheets providing the reference results.

2. Materials, samples and methods

2.1. Manufacturing of laminates

For this study five types of laminates were thermoformed from two consolidated plies of glass roving–PA6 (thermoplastic-based) organo sheets with a woven architecture (2×2 twill). Both plies were laid such that the orientation of the warp and weft yarns matched. Further in the text, such a laminate will be called 0˚-laminate. For the other four types, the laminates in the hot state were sheared to various angles: 15˚, 30˚, 45˚ and 60˚, using a picture frame setup and then consolidated (Fig. 1).

2.2. Tensile testing

Using a waterjet, samples were cut from the laminates in two different positions, namely, in the bias direction (Position 1) and in the warp direction (Position 2) (red rectangles in Fig. 1). Tensile tests were performed according to the ISO 527-5 using a universal testing machine Zwick with the test speed 5 mm/min. The tests were accompanied by a mechanical and optical (digital image correlation (DIC)) extensometer. The modulus of elasticity was calculated as a slope of the stress-strain curve between 0.05 and 0.2% strain.

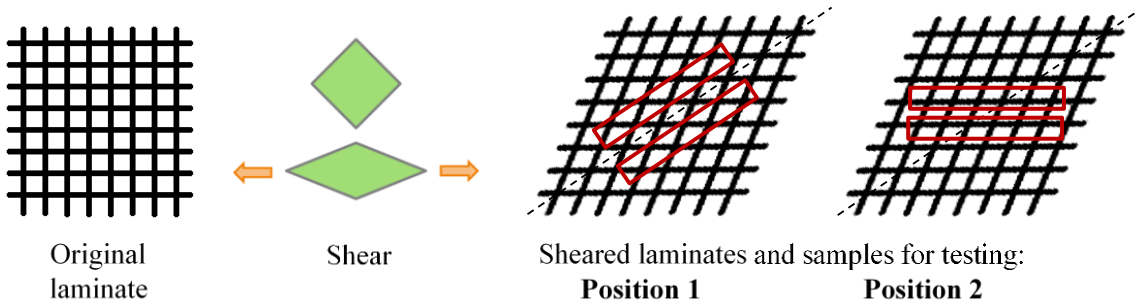

Figure 1. Schematics showing shear of the organo sheets-based laminates and sample extraction for the tensile tests (in red).

2.3. Micro-CT imaging and image segmentation

One specimen for each laminate type was cut from the plates using a band saw. The samples were taken in the bias direction (Position 1, Fig. 1) and such that they contain a woven fabric repetitive unit cell. All of the specimens had approximately equal areal dimensions of 2.6×4.5 cm^2. The thickness of the laminates was preserved. The specimens were scanned with the voxel size of 14.56 µm by XRE NV (Belgium) using their UniTOM X-ray computed tomography system. Reconstructed cross-sectional images through the sample thickness are shown in Fig. 2.

Next, the 3D micro-CT images were used to recreate voxel-based geometry of the samples using VoxTex software (MTM, KU Leuven) [4, 5, 10]. For that purpose, the image stacks were divided into cubic sub-volumes with the edge of 116.48 µm (so-called voxels[1]) followed by segmentation into components (material features) of the voxel model. In this work, only three components were

[1] The reader should not mistake this “voxel” (a sub-volume) with a “voxel” of the CT images. A sub-volume is made of multiple CT voxels. It is also reflected in the size difference: 116.48 µm vs. 14.56 µm. Later in the paper, the term “voxel” will be used in the sub-volume meaning.

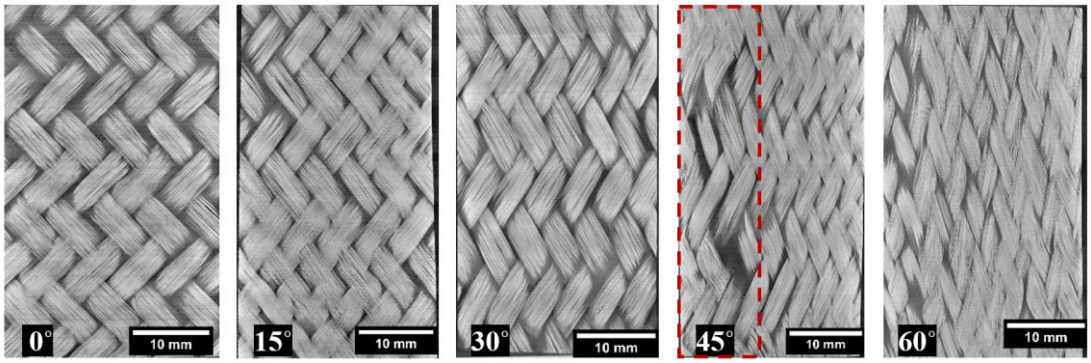

Figure 2. Micro-CT images of the sheared organo sheet laminates (2×2 twill), cross-sections through the laminate thickness. Degrees denotes the shear angle. The dashed red rectangle indicates a defect in 45˚-laminate.

considered, namely, matrix, warp and weft yarns. Voids were not taken into account as a separate material component, because their dimensions were much smaller than the sub-volume size. However, the presence of voids was introduced to the FE models via the corrected fiber volume fraction. The segmentation was done using three feature variables: average grey value (density), structural anisotropy and azimuthal orientation angle in the spherical coordinates. The last parameter drives the distinction of yarns of the warp and weft directions.

One can notice that the 45˚-laminate contained internal defects, i.e. big voids and yarn misalignments (red rectangle, Fig. 2), which may be present in real materials. However, this defect was not taken into account in the modeling. The defective volume was cropped from the studied volume to allow following the same image segmentation procedure for all the laminates.

2.4. Finite element modeling for numerical homogenization

Model Generator Engine (MGE) was developed and implemented in Siemens PLM Software to form a link between VoxTex and Simcenter FE environment including VMC ToolKit. The latter is a set of software tools developed for virtual material characterization (VMC) [11] in order to replace physical tests with virtual experiments and to estimate the “as-manufactured” properties of specimens in a fast and reliable manner. The VMC ToolKit allows obtaining homogenized material properties at different scales: micro-scale to predict properties of impregnated yarns and subsequently linked to meso-scale and obtain the homogenized material properties of composite plies.

In this work, the input model is a voxel model automatically created in Simcenter from a VoxTex output file using MGE. These models include material components and local material orientations. The workflow is depicted in Fig. 3 and was followed to build five FE models of the studied laminates.

In modeling of the specimens elastic response, the plane stress assumption was accepted, because the thickness of the studied laminates was much smaller than their two other dimensions. Thus, only three loading cases were solved to obtain the in-plane laminates homogenized elastic properties. These cases were tension in the X- and Y-directions and simple shear XY, considering that the laminates lied in the XY plane (Fig. 3).

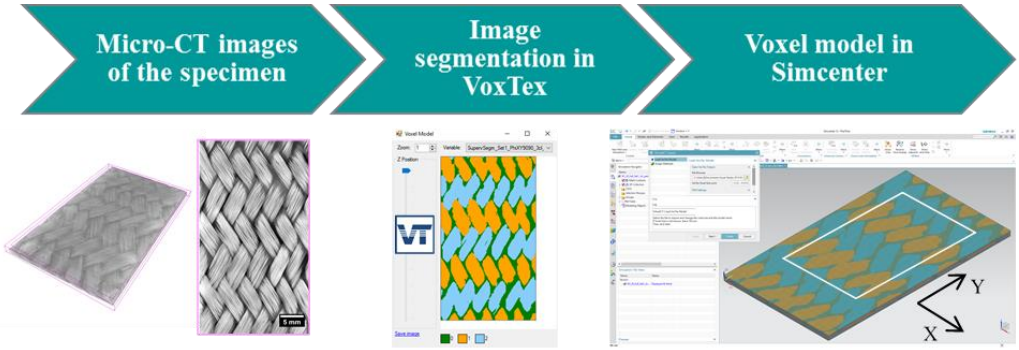

Figure 3. MGE workflow by an example of the 30˚-laminate. Green, yellow and blue colors represent a matrix, yarns of the warp and weft directions respectively. Local orientation vectors are specified in each voxel. A unit cell is shown in the white rectangle.

Micro-CT-based voxel models have weak periodicity on the boundaries. Consequently, the usage of the periodic boundary conditions is not straightforward [5]. As a solution, Straumit in [5] suggested to use Dirichlet boundary conditions. They were also used in this work and applied on the specimen edges, except the top (Z = thickness) and bottom (Z = 0) surfaces which were left unconstrained. In addition, four corner nodes of the bottom surface were fixed in the Z-direction to prevent the vertical movement of the model.

Materials used in the calculations were PA6 matrix with the density of 1140 kg/m^3, the elastic modulus of 2.28 GPa and Poisson's ratio of 0.38, and a glass fiber with the density of 2540 kg/m^3, Young's modulus of 70 GPa and Poisson's ratio of 0.22 [12]. Fiber volume fraction (VF) inside the yarns was calculated for each laminate type based on the measurements of samples weight and dimensions and the analysis of void content (see sections 3.1 and 3.2).

FE models were solved with Siemens PLM Software structural solver for linear static analysis. Numerical homogenization was performed on several unit cells which were a subset of the complete modeled specimen volume (right image, Fig. 3).

3. Results and discussions

3.1. Void content analysis

The produced laminates were not free of defects. Pores were present in all of them, which can be seen in Fig. 2. Their amount was assessed using a void content analysis tool of VoxTex. A threshold was applied to the CT images to segment them into voids (black) and solid materials (white), then the ratio of black CT voxels to the sample volume was calculated. The resulting porosity levels are the following: for the 0˚-laminate – 4.9%, for the 15˚-laminate – 3.6 %, for the 30˚-laminate – 8%, for the 45˚-laminate – 5.1% and for the 60˚-laminate – 1%.

The lowest void content was found in the 60˚-laminate, which can be explained with an extra pressure created due to a large shear angle applied at the production step. The higher pressure helped a better fiber impregnation and filling up resin-free zones between the yarns. For the rest of the laminates, it is difficult to define a trend between the shear angle and void content. Based on the voidage values and the micro-CT images, it can be concluded that the manufacturing pressure was not sufficient to eliminate resin-starved areas between the yarns.

3.2. Calculation of fiber volume fraction

In order to determine the actual fiber VF for each laminate type, the scanned specimens were weighted with a precision lab balance, and their dimensions were measured with a caliper. The density of the

specimens was determined by finding their weight-to-volume ratio. Such a density definition does not consider pores present in the volume. However, the micro-CT images revealed the opposite. In section 3.1, the void content was determined for each studied sample. Thus, another density calculation was performed to take the voids volume into account. The volume of pores was deducted from the specimens volume and, then, the weight-to-volume ratio was again estimated. Afterward, the fiber VF was assessed using Eq. 1:

$$VF_f = (\rho_c - \rho_m) / (\rho_f - \rho_m), \quad (1)$$

where ρ_c is the calculated density of the composite laminate (with or without pores), ρ_m is the density of PA6 (1140 kg/m^3), and ρ_f is the density of the glass fiber (2540 kg/m^3) [12]. The resulting fiber VF's are shown in Fig.4 and indicate a strong variability from sample to sample.

To check the sensitivity of the recalculated fiber VF's to the density of PA6 matrix, the latter was varied in the range of 1000 – 1300 kg/m^3, a typical range for PA6, which can be found in literature [12]. The density of the glass fiber was assumed to be unchanged and equal to 2540 kg/m^3. The results of this sensitivity tests are presented in Fig.4 as error bars from the calculated VF's.

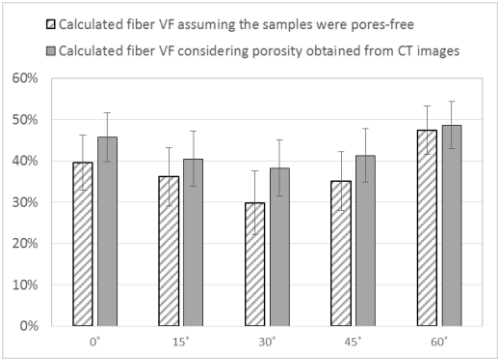

Figure 4. Calculated fiber volume fractions (VF's) in the studied laminates, which were obtained assuming no porosity in the samples volume and considering porosity levels found from the analysis of the micro-CT images. Error bars indicate the VF's sensitivity to the matrix density.

3.3. Results of the tensile tests

The elastic moduli measured in the tensile tests with the use of a mechanical extensometer and DIC are depicted in Fig. 5. Generally, the test results indicate a wider scatter of the modulus values for strain measured with the extensometer. One explanation could be the growing out-of-plane deformations as a function of the applied force. Thus, reading the extensometer measurements becomes challenging. The strain was also calculated using DIC. Two cameras were used to capture out-of-plane deformations which could be of the same order as the in-plane deformation. Separating strain components with DIC is assumed to contribute in reducing the modulus scatter and in increasing the fidelity of the results. At higher degrees of shear (30˚, 45˚and 60˚), variability or even non-regularity of the internal structure is more pronounced than in composites with lower degrees of shear, which also results in a wider spread of the elastic modulus.

In the bias direction (Position 1), Young's modulus grows as a function of the shear angle (Fig. 5). Increasing the shear angle leads to the rotation of yarns in the bias direction and, consequently, more fibers become oriented in the loading direction increasing the modulus. In the warp direction (Position 2), the trend for the modulus follows the same trend as the fiber VF.

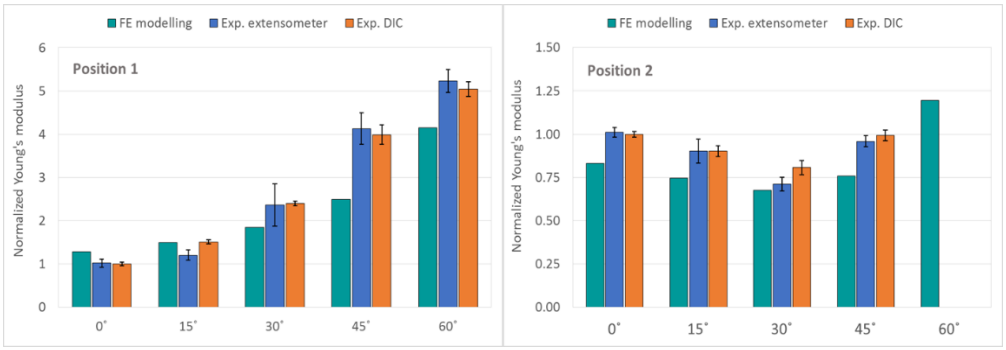

Figure 5. Normalized elastic modulus: experiments vs. FE predictions for the bias direction (Position 1) and the warp direction (Position 2). Normalization is done by the value of the elastic modulus of the 0˚-laminate measured in the experiments with DIC (orange color). For the 60˚-laminate, the warp direction was unfeasible to define due to a big distortion of the mesostructure, therefore the experimental values for Position 2 are missing.

3.4. Predicted homogenized elastic properties using FE analysis

Five voxel models were solved for the three loading cases. An example is shown in Fig. 6. FE homogenization was performed on a unit cell allowing an estimation of two in-plane Young's moduli (X- and Y-directions). The elastic modulus in the bias direction corresponded to the predicted value in the Y-direction. To obtain Young's modulus in the warp direction, the unit cell's compliance matrix has to be rotated by a certain angle α towards the Y-direction, so that the warp yarns would become oriented along the Y-axis (Fig. 6).

In textile composites, the warp direction is always a little bit stiffer than the weft direction due to a lower crimp. Multiple rotations of the compliance matrix with the step of one degree were performed, and a set of the modulus values was obtained. Young's modulus in the warp direction was chosen as the largest modulus from this set, and the angle α (Fig. 6) corresponding to the maximum modulus was used to assess the actual shear angle of the fabric γ following Eq.2:

$$\gamma = 90^\circ - 2\alpha \tag{2}$$

Angle γ was found to differ by 5-7˚ from the nominal shear angles imposed on the organo sheets during manufacturing of the laminates with the exception of the 60˚-laminate (see Table 1).

Table 1. Assessment of shear angle.

Nominal shear angle imposed on the sheets, ˚	Estimated actual shear angle γ, ˚
0	4
15	10
30	24
45	52
60	84

The normalized homogenized moduli in the bias and warp directions are plotted against the experimental values in Fig. 5. The differences between numerical and experimental results are assumed to be due to

- *the variability in the material* (e.g. voids, change of the fiber VF and local thickness as a response to shear) and

- *the sample preparation* (e.g. a mismatch in the samples alignment, which were cut for the tensile tests and micro-CT scans). The modeling results indicate that changing the angle α (Fig. 6) by 10˚ may result in ~10% modulus difference.

The quantification of the material variability is out of the scope of the current work. A stochastic description of complex 3D textile architectures based on multiple unit cells can be found in [13].

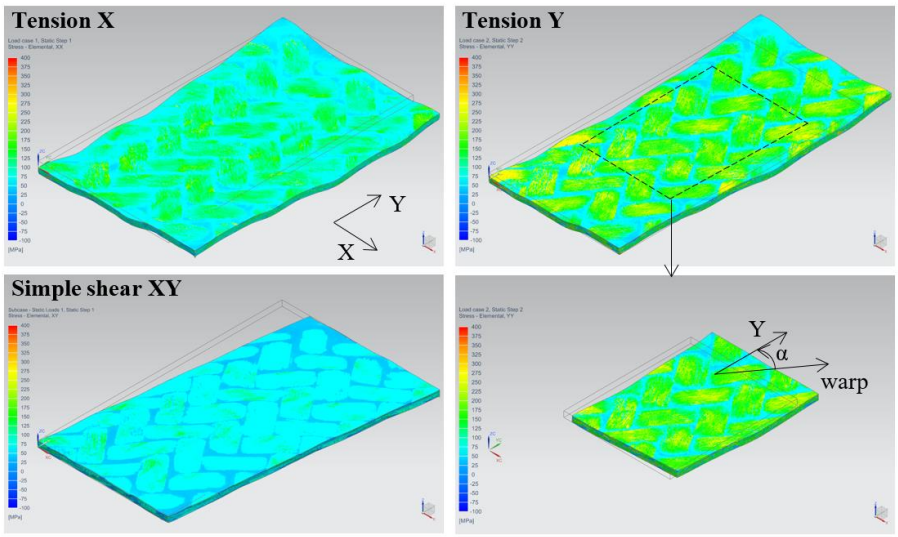

Figure 6. 15˚-laminate: stress distribution in three loading cases (tension in the X-direction, tension in the Y-direction and simple shear XY) and an example of a unit cell (tension in Y direction). Deformation scale is 10% of the model, which makes out-of-plane deformation more pronounced. The initial shape is shown as a wire frame.

3.6. Conclusions

The unit cell mesostructure of the sheared Glass Roving–PA6 consolidated composite plies was characterized using X-ray micro-computed tomography. 3D micro-CT images were used to create the voxel-based geometry of the unit cells using VoxTex software. To form a link between VoxTex and Simcenter FE environment, a Model Generator Engine was developed and implemented in Siemens PLM Software. This allowed a high-fidelity micro-CT-based reconstruction of the analyzed sheared organo sheets, capturing the variation yarn orientation and the thickness of the laminates.

A micro-CT-based FE-homogenization was, further, performed to compute the homogenized elastic properties of non-sheared and sheared organo sheets. First, properties of the yarns were homogenized on the microscale using analytical formulation, which were subsequently linked to the mesoscale. Homogenization on the mesoscale was performed assuming the plane stress condition with three in-plane load cases using Dirichlet boundary conditions. In order to build the stiffness matrix, homogenized stresses and strains were extracted from the periodic unit cell and averaged by volume. The effective elastic properties were determined and compared with the existing experimental data in the bias direction and along the warp direction. The error between the average experimental values and predicted Young's moduli lies in the range of 2-15% in the warp direction and in the range of 5-32% in the bias direction. The differences are assumed to be due to the variability in the material and in the sample preparation and testing processes.

The proposed enrichment of the VMC ToolKit with a link to micro-CT provides an industry-ready solution that supports the understanding of the structural features of composite materials, their influence on materials' performance and changes in those features during composites' manufacturing and eventually exploitation.

Acknowledgments

The authors gratefully acknowledge SIM (Strategic Initiative Materials in Flanders) and VLAIO (the Agency Flanders Innovation & Entrepreneurship) for their support of the IBO project M3Strength (Grant no.140158), which is part of the research program MacroModelMat (M3). O. Shishkina thanks VLAIO for financing her work in the framework of the Innovation Mandate Project "MicroCT-based Model Generation Engine for Virtual Material Characterisation" (Grant no. HBC.2017.0189). S.V. Lomov holds Toray Chair for Composite Materials at KU Leuven, the support from which is also acknowledged.

References

[1] Van Mieghem, B. An intelligent experimental approach for the optimisation of the process parameters for the thermoforming of plastics and composites, PhD thesis. University of Leuven (KU Leuven), Leuven, Belgium. 2015

[2] Vanclooster, K. Forming of multilayered fabric reinforced thermoplastic composites. PhD thesis. University of Leuven (KU Leuven), Leuven, Belgium, 2009.

[3] A. Matveeva, L. Farkas, G. Gruber, S. Wiedemann, S. Lomov, T. Analytical and numerical characterization of sheared organo sheets, *Proceedings of the 8th International Conference on Composites Testing and Model Identification*, Leuven, 2017.

[4] Straumit, I., S.V. Lomov and M. Wevers, Quantification of the internal structure and automatic generation of voxel models of textile composites from X-ray computed tomography data. *Composites Part A*, 54:150-158, 2015.

[5] Straumit I. Prediction of the effective properties of textile composites based on X-Ray computed tomography data. PhD thesis. University of Leuven (KU Leuven), Leuven, Belgium. p.144, 2017.

[6] G. Harjkova, M. Barburski, S.V. Lomov, O. Kononova, I. Verpoest, Weft knitted loop geometry of glass and steel fiber fabrics measured with X-ray micro-computer tomography, *Text. Res. J.* 84(5): 500-512, 2014.

[7] D.J. Bull, S.M. Spearing, I. Sinclair, Observations of damage development from compression-after-impact experiments using ex situ micro-focus computed tomography, *Composites Science and Technology* 97: 106-114, 2014.

[8] Y. Swolfs, H. Morton, A.E. Scott, L. Gorbatikh, P.A.S. Reed, I. Sinclair, S.M. Spearing, I. Verpoest, Synchrotron radiation computed tomography for experimental validation of a tensile strength model for unidirectional fibre-reinforced composites, *Compos. A, Appl. Sci. Manuf.* 77:106-113, 2015.

[9] Y. Liu, I. Straumit, D. Vasiukov, S.V. Lomov, S. Panier, Multi-scale material model for 3D composite using Micro CT Images geometry reconstruction, *Proceedings of the 17th European Conference on Composite Materials ECCM-17*, Munich, 26-30 June 2016

[10] I. Straumit, I. Baran, L. Gorbatikh, L. Farkas, C. Hahn, K. Ilin, J. Ivens, L. Lessard, Y. Liu, N. Nguyen, A. Matveeva, M. Mehdikhani, O. Shishkina, J. Soete, J. Takahashi, D. Vandepitte, D. Vasiukov, Y. Wan, E. Winterstein, M. Wevers, S. V. Lomov, Micro-CT-based analysis of fibre-reinforced composites: applications, *Proceedings of the 18th European Conference on Composite Materials ECCM-18*, Athens, 24-28 June 2018

[11] L. Farkas, K. Vanclooster, H. Erdelyi, R. Sevenois, S. Lomov, T. Naito, Y. Urushiyama, W. Van Paepegem, Virtual material characterisation process for composite materials: an industrial solution, *Proceedings of the 17th European Conference on Composite Materials ECCM-17*, Munich, 26-30 June 2016, paper 3.05-20

[12] Material Property Data, MatWeb, http://www.matweb.com/

[13] A. Vanaerschot, F. Panerai, A. Cassell, S.V. Lomov, D.Vandepitte, N.N. Mansour. Stochastic characterisation methodology for 3-D textiles based on micro-tomography. *Composite Structures* 173: 44–52, 2017.